# Ribosome Biogenesis Is Sensed at the Start Cell Cycle Checkpoint⊡

## Kara A. Bernstein,* Franziska Bleichert,* James M. Bean,† Frederick R. Cross,†‡ and Susan J. Baserga*‡§∥

Departments of §Molecular Biophysics and Biochemistry, *Genetics, and ∥Therapeutic Radiology, Yale University School of Medicine, New Haven, CT 06520; and †Rockefeller University, New York, NY 10021

In the yeast *Saccharomyces cerevisiae* it has long been thought that cells must reach a critical cell size, called the "setpoint," in order to allow the Start cell cycle transition. Recent evidence suggests that this setpoint is lowered when ribosome biogenesis is slowed. Here we present evidence that yeast can sense ribosome biogenesis independently of mature ribosome levels and protein synthetic capacity. Our results suggest that ribosome biogenesis directly promotes passage through Start through Whi5, the yeast functional equivalent to the human tumor suppressor Rb. When ribosome biogenesis is inhibited, a Whi5-dependent mechanism inhibits passage through Start before significant decreases in both the number of ribosomes and in overall translation capacity of the cell become evident. This delay at Start in response to decreases in ribosome biogenesis occurs independently of Cln3, the major known Whi5 antagonist. Thus ribosome biogenesis may be sensed at multiple steps in Start regulation. Ribosome biogenesis may thus both delay Start by increasing the cell size setpoint and independently may promote Start by inactivating Whi5.

## INTRODUCTION

Ribosome biogenesis is a highly coordinated and complex process that requires over 200 nonribosomal proteins and many small nucleolar RNAs (snoRNAs). Synthesis of the 35S pre-rRNA, which gives rise to three of four mature rRNAs (18S, 25S, and 5.8S rRNAs), begins in the cell nucleolus. Many processing and modification steps on the pre-rRNA lead to the mature 18S that becomes incorporated into the small ribosomal subunit (SSU) and the 25S and 5.8S rRNAs that are incorporated into the large ribosomal subunit (LSU). The 5S rRNA, the final rRNA component of the LSU, is transcribed and processed separately.

Processing of the pre-18S rRNA occurs via a large complex of more than 40 nonribosomal proteins and the U3 snoRNA termed the small subunit (SSU) processome/90S pre-ribosome (Dragon *et al.,* 2002; Grandi *et al.,* 2002; Schäfer *et al.,* 2003). This complex can be visualized in chromatin spreads as the knobs on the ends of the nascently transcribed pre-rRNAs (Dragon *et al.,* 2002; Gallagher *et al.,* 2004). Now that many components required for making ribosomes have been identified, recent work has focused on understanding how ribosome biogenesis is regulated and connected to other cellular processes including the cell cycle.

Recent work has shown a connection between ribosome biogenesis and the cell cycle. In yeast, depletion of SSU processome proteins leads to G1 delay and an inability to reenter the cell cycle (Bernstein and Baserga, 2004); other cell cycle defects upon inhibition of ribosome biogenesis in yeast have been observed (Du and Stillman, 2002; Oeffinger and Tollervey, 2003; Jorgensen *et al.,* 2004a; Saracino *et al.,* 2004). In animal cells, removal of *BOP1*, which is required for pre-rRNA processing of the LSU pre-RNAs, leads to G1 arrest (Pestov *et al.,* 2001a, 2001b; Strezoska *et al.,* 2002). Still, the mechanisms coordinating ribosome biogenesis and cell cycle are largely unknown.

Cell growth and division are coordinated processes in which cells must reach a critical size before cell division can occur. Classical studies defined a critical cell size or "setpoint" required for progression at Start, the point at which cells commit to cell division during late G1 (Hartwell *et al.,* 1974; Johnston *et al.,* 1977). Similar phenomena exist in a wide variety of organisms including bacteria, fission yeast, and avian erythroblasts (Donachie, 1968; Hartwell *et al.,* 1974; Johnston *et al.,* 1977; Nurse and Thuriaux, 1977; Dolznig *et al.,* 2004). Arrest at Start in yeast can be caused by nutrient deprivation, mating pheromones, or translation defects (Unger and Hartwell, 1976; Hartwell and Unger, 1977; Johnston *et al.,* 1977). It is not known whether the critical cell size setpoint sensed corresponds to cell volume, protein content per cell, RNA content per cell, or rates of protein or ribosome synthesis (Jorgensen and Tyers, 2004).

Cln3, a G1 cyclin, functions by activating the SBF (Swi4-Swi6) and MBF (Mbp1-Swi6) complexes, which transcriptionally activate many genes involved in DNA synthesis and repair (Wijnen and Futcher, 1999). Cln3 may be important for cell size sensing at Start. Cln3 is highly unstable and may be a rate-limiting Start activator (Cross and Blake, 1993; Tyers *et al.,* 1993; Polymenis and Schmidt, 1997). Therefore, if translation is inhibited or ribosome levels decrease, then insufficient Cln3 protein might be available for the cell size setpoint and Start progression.

Recently, Whi5, a functional equivalent to human tumor suppressor Rb, has been identified as a key regulator of the yeast Start checkpoint (Costanzo *et al.,* 2004; de Bruin *et al.,* 2004; Jorgensen and Tyers, 2004). Whi5 negatively regulates passage through Start by inhibiting SBF and MBF activation and may itself be inhibited by Cln3-Cdc28–dependent phosphorylation.

Regulation of expression of the ribosome biosynthetic regulon (RiBi) and the ribosomal proteins themselves has recently been elucidated in yeast (Jorgensen *et al.,* 2002) with the discovery of two transcription factors, Sfp1 and Sch9, which function in the Ras/PKA and TOR signaling pathways to control the ribosome biosynthetic rate (Fingerman *et al.,* 2003; Jorgensen *et al.,* 2004a; Marion *et al.,* 2004). It has been proposed that expression of the RiBi regulon also affects the cell size setpoint for Start, because mutations that inhibit RiBi expression result in small cells passing Start (Jorgensen *et al.,* 2002; Jorgensen and Tyers, 2004). The mechanism by which this occurs is unknown but is thought to be independent of the main Start regulatory pathway (Cln3, Whi5, SBF/MBF, Cln1/2).

Here we show that cells respond to deficiencies in ribosome biogenesis by delaying Start, expanding the early G1 part of the cell cycle during which Whi5 is nuclear. This delay occurs before a decrease in overall levels of ribosomes, total protein levels, or protein synthesis; thus, cells may anticipate mRNA translation deficiencies before the changes actually occur. As a result, the Whi5 protein is retained in the nucleus where it may inhibit passage through Start. When the *WHI5* gene is disrupted, cells are unable to delay the cell cycle in response to changes in pre-rRNA levels, at least until overt ribosome depletion is detectable. In contrast, deletion of *CLN3*, the major Whi5 antagonist, has no effect on this mechanism. Our results suggest that ribosome biogenesis has a positive effect on Start and that when ribosome biogenesis is defective, Whi5 is retained in the nucleus. Combined with evidence that ribosome biogenesis may delay Start by increasing the cell size setpoint (Jorgensen *et al.,* 2004), we conclude that ribosome biogenesis is sensed at multiple steps in Start regulation.

## MATERIALS AND METHODS

### Yeast Strains and Media

Yeast strains were derived from YPH499 (Mat**a**, *ura3-52, lys2-80, ade2-101, trp1-Δ63, his3-Δ200, leu2-Δ1*). *GAL-3xHA-PWP2* Whi5-GFP and Whi5-GFP yeast strains were derived from W303. Yeast was grown in rich medium YPD (1% yeast extract, 2% peptone, 2% dextrose), YPG/R (1% yeast extract, 2% peptone, 2% galactose, 2% raffinose), SC (synthetic complete) media with either -D (2% dextrose) or -G (2% galactose) and minus uracil (-URA) where specified. Yeast with C-terminal 3xHA-tagged proteins or N-terminal GAL-3xHA–tagged proteins were created (Longtine, 1998). Yeast expressing Cln3-HA-MYC (TRP marker) was genomically integrated with the pMM162 plasmid from Mary Miller (Miller *et al.,* 2005). *WHI5* and *CLN3* disruptions were made using the CLONAT (pAG25) marker (Goldstein and McCusker, 1999).

### Growth Curves

Cells were grown in YPG media to early log phase and then shifted into YPD media for 24 h. Cells were maintained in early log phase throughout the time course and analyzed for growth by measuring absorbance at $OD_{600}$ or $OD_{660}$; the percentage unbudded and DNA content were measured by flow cytometry on a FACSCalibur System (BD Biosciences, San Jose, CA) or cell size by Beckman Coulter counter Model Z2 (Fullerton, CA).

### Vacuole Staining

YPH499 and *GAL::3xHA-PWP2* were grown to early log phase in SC-G media. Cells were shifted into SC-D media for 21 h to an $OD_{600}$ of 0.4. One milliliter of cells was gently sonicated, and 40 $\mu$m of FM4-64 (Molecular Probe T3166) was added. Cells were incubated for 1 h at 30°C, washed with SC-D, and fixed to a slide in 0.6% LMP agarose and visualized on a Zeiss Axioplan2 microscope (Thornwood, NY).

### Time-Lapse Microscopy

Yeast strains expressing Whi5-GFP (Costanzo *et al.,* 2004), *PWP2* or *GAL::3xHA-PWP2,* were grown in SC-G media to early log phase, then shifted to SC-D media for 4, 5.5, or 7 h, and then analyzed by time-lapse microscopy as previously described (Bean *et al.,* 2006). Fluorescent and phase-contrast images were acquired at 3 min resolution for 9 h. Only a subset of yeast was included in the analysis because of unscorable faint/undetectable Whi5-GFP expression or out-of-plane bud emergence.

### Protein Analysis by Western Blot

Yeast with Pwp2-3xHA, *GAL::3xHA-PWP2,* or *GAL::3xHA-PWP2/*Cln3-HA-MYC were grown to early log phase in YPG. Cells were shifted into YPD or YPG media and maintained at an $OD_{600}$ of 0.3–0.6. Equal numbers of cells were collected at either 0, 4, 8, 10, 12, 14, 16, 20, or 24 h of growth in YPG or YPD, and protein was extracted as previously described (Kushnirov, 2000). Protein was analyzed by 10% SDS-PAGE and Western blotted either with anti-HA antibodies (12CA5) to detect Pwp2, anti-Mpp10 antibodies to detect Mpp10 (Dunbar *et al.,* 1997), anti-Myc antibodies to detect Cln3 (9E10) or anti-Adh1 antibodies (Chemicon, Temecula, CA; Ab1202) to detect the alcohol dehydrogenase protein (1:1500) as previously described (Bernstein and Baserga, 2004; Bernstein *et al.,* 2004).

### Cell Elutriation

One liter of YPH499, *GAL-3xHA-PWP2, whi5Δ, GAL-3xHA-PWP2 whi5Δ* yeast were grown to early log phase in YPG/R media and then shifted into YPD media for 12 h. Yeast were sonicated in 75 ml of ice-cold water for 3 min total. Cells were elutriated (Beckman J-6M/E centrifuge, Fullerton, CA) at 4°C in cold water at 3000 RPM, and 12 fractions of 400 ml were collected and analyzed for percentage unbudded, DNA content, RNA content, and protein content as described below. Pump speeds varied by elutriation, but all were increased by 10% with each collected fraction.

### RNA and Protein Analysis from Elutriated Fractions

For RNA analysis, 15 ml from each fraction was collected and washed two times with 1× PBS. Cells were resuspended in 0.5 ml Tris-HCl, 7.5 (200 mM)/NaCl (211 mM)/MgCl$_2$ (78 mM), and 55 $\mu$l of propidium iodide (1 mg/ml). For protein analysis, equal numbers of cells from each fraction were collected and washed twice in 1× PBS. Cells were resuspended in 0.5 ml sodium bicarbonate (0.5 M) and 25 $\mu$l of fluorescein isothiocyanate (FITC; 1 g/l) were added, and cells were incubated on ice for 30 min. Cells were washed twice with 1× PBS, resuspended in 0.5 ml 1× PBS, and analyzed as described (Popolo *et al.,* 1982).

### RNA Analysis by Northern Blot

YPH499 or *GAL::3xHA-PWP2* were grown to early log phase in YPG/R media and shifted into YPD media for up to 24 h. RNA was extracted from yeast from 25 ml of culture grown to an $OD_{600}$ of 0.4 in YPD media for either 0, 4, 8, 12, 16, 20, or 24 h. Twenty micrograms of RNA was run on 1.25% agarose-formaldehyde gels as previously described (Lee and Baserga, 1999). To determine the 25S/18S ratios, 10 $\mu$g of RNA was run on a 1.25% agarose gel, stained with ethidium bromide, and analyzed using an Alphaimager 2200 (Alpha Innotech Corporation, San Leandro, CA). To quantitate the pre-rRNAs, the Northern blots were analyzed using a phosphoimager (Molecular Dynamics, Storm 840, Sunnyvale, CA).

### Metabolic Labeling of RNA

YPH499 or *GAL::3xHA-PWP2* containing pGAD3 uracil-based plasmid was grown to early log phase in SG/R-URA media for 48 h and shifted into SD-URA media for 9 or 12 h. Forty milliliters of cells at OD600 0.4–0.5 was then pulsed for 2 min with 100 $\mu$Ci of [³H]uracil. RNA was extracted, and 20,000 cpm was analyzed as previously described (Dunbar *et al.,* 1997).

### Metabolic Labeling of Proteins

For quantitative analysis of new protein synthesis, YPH499 and *GAL::3xHA-PWP2* cells were grown in SG/R-MET medium and, except for the 0-h time point, shifted into SD-MET medium for 8, 10, 12, 16, and 24 h. Similar to growth in rich medium, growth of Pwp2-depleted cells was not affected until 12 h after the switch into dextrose-containing medium. We verified that the percentage of unbudded cells was already markedly increased by 8 h of Pwp2 depletion (data not shown). For metabolic labeling of proteins, 1 ml of cells of an OD600 0.5 was pelleted and resuspended in 1 ml SD-MET (8-, 10-, 12-, 16-, and 24-h time points) or SG/R-MET (0-h time point). After incubation at 30°C for 10 min, 3 $\mu$Ci of Tran³⁵S-label (MP Biomedicals, Solon, OH; 1175 Ci/mmol, 10.5 mCi/ml) were added. After 5 min labeling at room temperature, 400 $\mu$l of ice-cold chase buffer (21 mM cold methionine, 32% trichloroacetic acid [TCA]) was added, and cells were incubated at 65°C for 20 min. Cells were collected on GF/C filter paper using a Millipore (Bedford, MA) 1225 Sampling Manifold, washed three times with 5 ml ice-cold 5% TCA, and then washed three times with ice-cold 100% ethanol. GF/C filter papers were dried at room temperature, and the ³⁵S incorporation was measured in a scintillation counter.

Two milliliters of cells from YPH499, *GAL::3xHA-PWP2*, *whi5Δ*, and *whi5Δ GAL-3xHA-PWP2* were collected from early log phase cultures of yeast strains grown in YPG/R and shifted into YPD for 0, 3, 4, 6, 8, 9, 12, or 24 h. Samples were prepared and analyzed as previously described (Burton and Solomon, 2000).

## RESULTS

### Cells Depleted of Pwp2 Exhibit G1 Delay before Evident Growth Rate Decreases

Previously, we have shown that depletion of SSU processome proteins leads to inhibition of exit from G1 (Bernstein and Baserga, 2004). To examine this phenomenon further, we chose to study Pwp2/Utp1 as a representative of SSU processome components (Dragon *et al.,* 2002; Dosil and Bustelo, 2004; Gallagher *et al.,* 2004). For simplicity, we will refer to Pwp2/Utp1 by its original name, Pwp2. To deplete cells of Pwp2, we used a previously characterized strain (*GAL::3xHA-PWP2*) where Pwp2 is under control of a galactose-inducible (expressed; YPG/R) or dextrose-repressible (repressed; YPD) promoter. Western blot analysis demonstrated greatly reduced Pwp2 levels after 4 h in dextrose that became undetectable by 8–12 h (Figure 1A). In contrast, yeast where Pwp2 has only an epitope 3xHA tag (Pwp2-3xHA) did not reduce Pwp2 levels in dextrose. Similarly, levels of Adh1, an unrelated abundant protein, were not affected upon Pwp2 depletion (Figure 1A).

When *GAL::3xHA-PWP2* cells were shifted into YPD media, a significant slowing in growth as measured by OD600 was not observed until 12 h in dextrose (Figure 1B). At 8 h, both Pwp2-depleted and parent YPH499 cells are still growing at approximately the same rate. Because depletion of SSU processome proteins has previously been shown to cause a G1 delay by fluorescence-activated cell sorting (FACS; Bernstein and Baserga, 2004), cells were also analyzed for accumulation of unbudded cells, a different assay for G1 delay. Cells depleted of Pwp2 start to accumulate unbudded cells as early as 8 h after the switch to dextrose, indicating a delay in G1 (Figure 1B). Therefore, yeast depleted of Pwp2 have reduced Pwp2 protein levels at 4 h (Figure 1A), accumulated unbudded cells at 8 h but only significantly slow growth by 12 h in dextrose (Figure 1B; summarized in Figure 7). Throughout our experiments, we compared the effects of Pwp2 depletion in the *GAL::PWP2* strain to the parent strain, YPH499, both grown in dextrose, and not to *GAL::PWP2* nondepleted yeast grown in galactose. This is because it is most accurate to compare yeast grown in the same carbon source as it influences cellular growth rate, the percentage of unbudded cells, and cell size.

Previous work suggested that blocking ribosome biogenesis should lower the cell size setpoint for Start, resulting in passage of Start at smaller cell volumes (Jorgensen *et al.,* 2004a). Therefore, we asked whether cells depleted of Pwp2 were altered in size. We directly measured cell volume using a Coulter counter over the same time period in dextrose (Figure 1B). Surprisingly, when measured at 24 h of depletion, cells depleted of Pwp2 were larger than wild-type cells (Figure 1B).

### Cells Depleted of Pwp2 Bud at Larger Cell Size than Nondepleted Yeast with Moderately Reduced Cellular RNA Content

We asked whether the increase in cell size observed entails a parallel increase in cellular RNA and protein content. To do this, we analyzed yeast RNA and protein content per cell volume when Pwp2 is depleted. Cell cultures were fraction-

ated by elutriation, a method that creates a gradient of cells that are collected as fractions based on size. The smallest cells often correspond to unbudded G1 cells and are collected in the first fractions. The larger cells frequently correspond to budded cells and are collected in subsequent fractions. Thus, yeast of similar sizes and budding indices can be compared for RNA or protein content per cell volume.

Cell elutriation was used to sort yeast depleted of Pwp2 for 12 h, because it is the time at which growth is significantly slowed (Figure 1C). We confirmed that *GAL::PWP2-depleted* yeast were larger (Figure 1B) by analyzing elutriated fractions with cells at a budding index of 50%, which was used here as a reference point. At this budding index, *GAL::PWP2* cells had a modal cell volume of 50 fl, whereas the parent cells (YPH499) had a volume of 34 fl (Figure 1C; Supplementary Table 1). These results suggest that Pwp2-depleted yeast may have a larger critical volume for budding than wild type.

Elutriated yeast depleted or not of Pwp2 were analyzed for total RNA and protein content per cell volume. Total RNA was determined by single-cell assay using propidium iodide staining followed by FACS (see *Materials and Methods*). Protein content was determined by single-cell assay using FITC staining followed by FACS (Popolo *et al.,* 1982). To compare the results between cells depleted or not of Pwp2, we used a reference point of an elutriated fraction with 50% budded cells. Cells depleted of Pwp2 (50 fl) had a mode value of 441 RNA and 477 protein units (arbitrary units), whereas nondepleted cells (34 fl) had a mode value of 592 RNA and 421 protein units (Figure 1C; Supplementary Table 1). These results indicate that although cells depleted of Pwp2 are larger by volume according to the Coulter counter, they have less RNA content than nondepleted yeast.

### Yeast Depleted of Pwp2 Have Enlarged Vacuoles

One explanation for the increased volume of *GAL::PWP2* cells without an increase in protein or RNA content could be an increase in the size of the vacuole. Yeast depleted or not of Pwp2 for 21 h were analyzed by differential interference contrast (DIC) microscopy and with the vacuole stain, FM4-64, which intercalates into the membrane of the vacuole (Figure 1D). Microscopy indicated that yeast depleted of Pwp2 had evidently larger vacuoles than nondepleted cells (Figure 1D).

### Cells Depleted of Pwp2 Accumulate pre-rRNAs before a Decrease in the Levels of 18S rRNA

Pwp2 was previously found to be required for pre-rRNA processing of precursors to the 18S rRNA (Dragon *et al.,* 2002; Dosil and Bustelo, 2004; Gallagher *et al.,* 2004). We wanted to determine if the resultant pre-rRNA processing defects parallel the cell cycle changes we observed. Northern blot analysis of pre-rRNAs from cells depleted of Pwp2 showed that Pwp2-depleted yeast accumulated the 35S and 23S pre-rRNAs and decreased the 27SA2 and 20S pre-rRNAs beginning at ~8 h after depletion (Figure 2, A and B; summarized in Figure 7). This effect was more pronounced after 12 h of depletion, when the growth rate was significantly decreased (Figure 2B; summarized in Figure 7). Because the levels of the 25S rRNA are not affected by Pwp2 depletion (Dragon *et al.,* 2002; Dosil and Bustelo, 2004), we compared the ratio of the levels of the 35S and 20S pre-rRNAs to the 25S rRNA throughout the time course. These effects are quantitated in Figure 2C, where the 20S/25S ratio and the 35S/25S ratio clearly show that the 20S pre-rRNA decreases and 35S pre-rRNA accumulates beginning no later than 8 h after the shift to dextrose medium. Because pre-rRNAs began to accumulate, indicating defects in ribosome biogene-
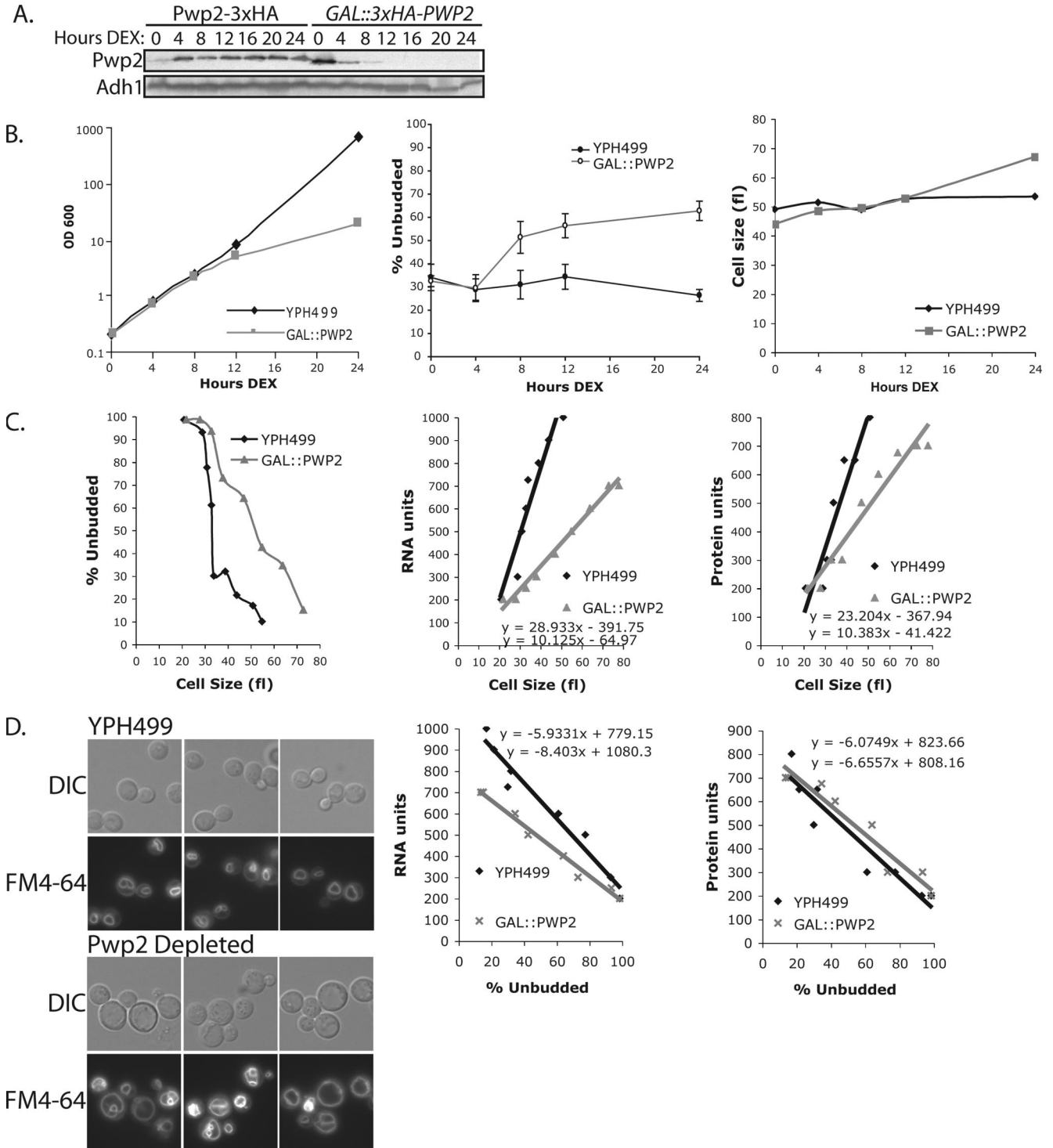
**Figure 1.** Yeast depleted of Pwp2 accumulate unbudded cells and bud at a larger cell size. (A) Protein levels of Pwp2 decrease by 4 h of depletion. *GAL::3xHA-PWP2* or Pwp2-3xHA yeast were grown to early log phase in YPG and then shifted into YPD. Equal amounts of cells were collected, and protein was extracted and analyzed by Western blot for Pwp2 (anti-HA antibodies) or Adh1 (anti-Adh1 antibodies). (B) Cell growth, percentage of unbudded cells, and cell size were monitored in Pwp2-depeleted yeast. *GAL::PWP2* and the parental strain (YPH499) were grown in YPG media and shifted into YPD media. The percentage of unbudded cells was averaged from four independent experiments, and the SD is indicated. (C) Elutriation of Pwp2-depleted and nondepleted yeast. *GAL::PWP2* and YPH499 were grown in YPG media and then shifted into YPD media for 12 h. Yeast were elutriated and collected as fractions. Fractions were analyzed for percentage of unbudded cells versus cell size, RNA units versus percentage of unbudded cells, RNA units versus cell size (fl), protein units versus percentage of unbudded cells, and protein units versus cell size (fl). (D) Pwp2-depleted yeast have enlarged vacuoles. *GAL::3xHA-PWP2* and YPH499 were grown in SC-G and then shifted into SC-D media for 21 h. Cells were stained with vacuole stain FM4-64 and visualized by DIC or for FM4-64 staining on a Zeiss Axioplan2 microscope.
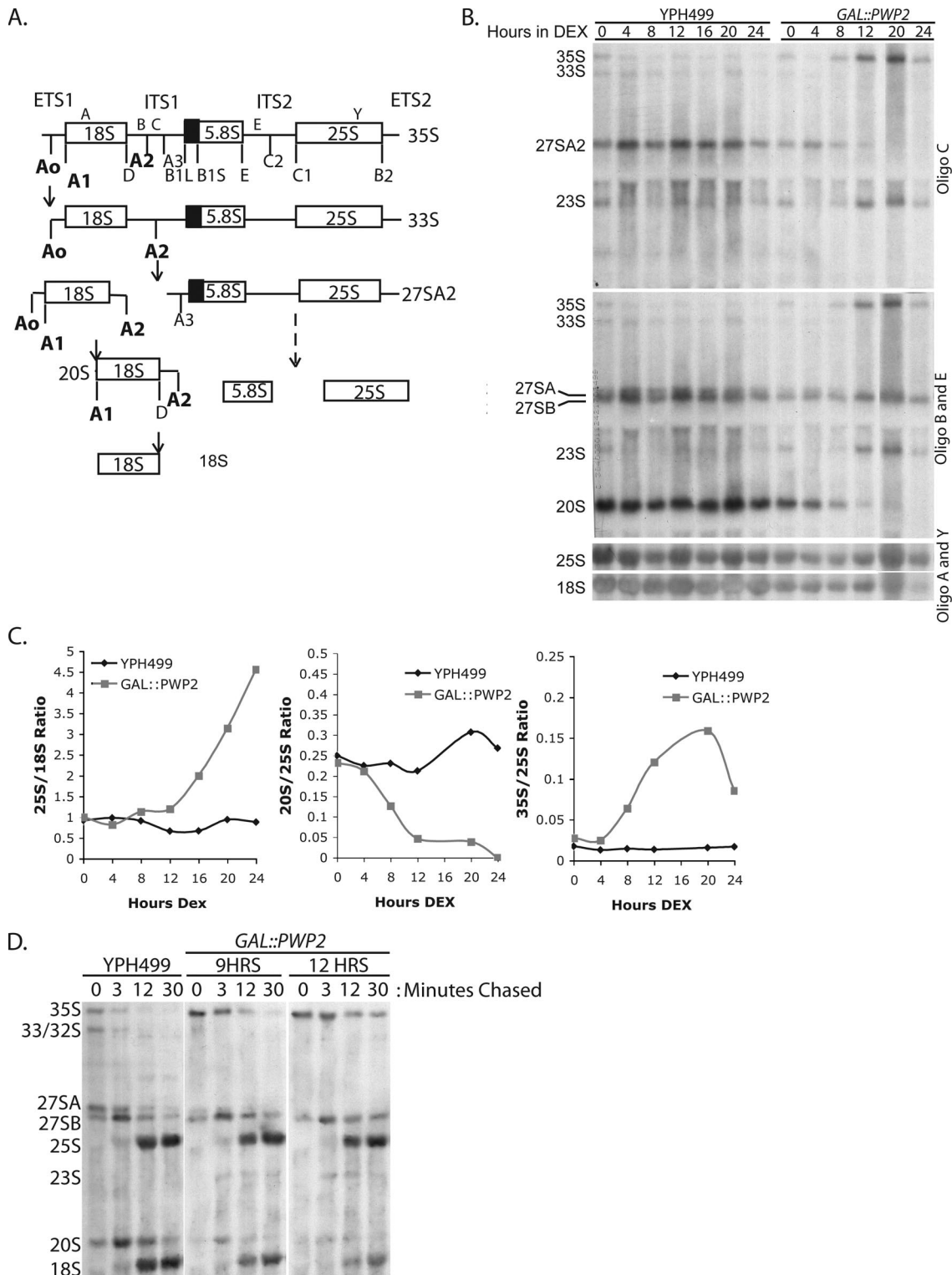
**Figure 2.** Cells depleted of Pwp2 accumulate pre-rRNAs before a decrease in 18S rRNAs levels. (A) Schematic of pre-rRNA processing in yeast. The SSU processome is required for pre-18S biogenesis at pre-rRNA processing sites A0, A1, and A2 (bold text). Oligos C, B, E, A, and Y were used as previously described (Lee and Baserga, 1997). Defects in these processing steps lead to accumulation of the 35S and 23S pre-rRNAs and a reduction in the 27SA2 and 20S pre-rRNAs and 18S rRNA. (B) Northern blot indicating that pre-rRNAs accumulate beginning at 8 h of Pwp2 depletion. Yeast depleted (*GAL::PWP2*) or not (YPH499) of Pwp2 were grown in YPG and shifted into YPD media. RNA was Northern blotted for pre-rRNAs and the mature 25S and 18S rRNAs. (C) Quantification of the results in B. Ratio of the 25S to 18S rRNAs (25S/18S ratio) were analyzed and plotted by time in YPD (Hours DEX) for *GAL::PWP2* and YPH499. Ratio of the 20S/25S and 35S/25S RNAs were analyzed and plotted by time in YPD (Hours DEX). (D) Metabolic labeling indicating pre-rRNA processing defects at 9 and 12 h of depletion. *GAL::PWP2* and YPH499 were grown in SG-URA and shifted into SD-URA media for 9 or 12 h. Cells were labeled with [³H]uracil and then incubated with complete media. RNA was extracted and equal counts were analyzed.

sis, after 8 h of Pwp2 depletion, we asked whether levels of the mature 25S and 18S rRNAs would also change after 8 h. When Pwp2 was depleted, the ratio of 25S/18S rRNA increased after ~12 h, indicating reduced 18S levels, which corresponded to the time when growth was significantly slowed (Figure 2C; see also Figure 7). In contrast, in nondepleted yeast grown in the same medium the ratio of 25S/18S rRNAs was approximately 1:1 throughout the time course (Figure 2C). Similarly, pre-rRNA processing defects were observed before changes in the ratio of 25S/18S rRNAs in Pwp2-depleted cells by others (Dosil and Bustelo, 2004). Therefore, the observed increase in unbudded cells indicating G1 delay at 8 h occurs before the steady state levels of the mature 18S rRNA is decreased and thus may be directly related to defects in new ribosome synthesis that can be observed at the same time.

### Nascent Ribosome Synthesis But Not Protein Synthesis Is Inhibited when Unbudded Cells Begin To Accumulate Due to Pwp2 Depletion

To further determine if nascent ribosome synthesis is inhibited at the time unbudded cells accumulate, processing of newly transcribed pre-rRNA was analyzed by metabolic labeling with [³H]uracil (Figure 2D). The *GAL::PWP2* strain or the parent strain (YPH499) were depleted of endogenous levels of uracil and shifted into dextrose media for 9 and 12 h. Yeast were subsequently labeled with [³H]uracil (which labels all nascently made pre-rRNA) and followed by 0-, 3-, 12-, or 30-min incubation in complete media containing uracil. The results indicate that at 9 h of Pwp2 depletion, cells exhibit defects in processing of the pre-18S rRNAs and accumulate the 35S and 23S pre-rRNAs, concomitantly reducing the 27SA pre-rRNA, the 20S pre-rRNA, and the mature 18S rRNA (Figure 2D). This confirms that there are pre-rRNA processing defects at early time points after Pwp2 depletion.

Because levels of the 18S rRNA are decreased by Pwp2 depletion, resulting in a decrease in the number of functional ribosomes, we asked whether new protein synthesis would also be affected after the shift to dextrose medium. *GAL::PWP2* and YPH499 yeast were analyzed for new protein synthesis by metabolic labeling with Trans³⁵S-label after growth in dextrose. TCA-precipitable proteins were collected on GF/C filter papers and the ³⁵S-amino acid incorporation measured in a scintillation counter. The results show that at 8 h of Pwp2 depletion new protein synthesis is not yet reduced (Figure 3). By 10 h after the switch into dextrose-containing medium, new protein synthesis was slightly reduced and thereafter steadily decreased with progressive time of Pwp2 depletion. Thus, at 8 h of Pwp2 depletion, when unbudded cells are already accumulated and pre-rRNA processing defect become apparent, protein synthesis is not yet decreased (Figure 3).

### Yeast Depleted of Pwp2 Exhibit G1 Delay Independently of Cln3 Protein Levels

Cln3 functions as a positive regulator for cell cycle progression at Start. Because Cln3 mRNA and protein levels are highly unstable (Tyers *et al.,* 1992; Cross and Blake, 1993) and therefore Cln3 translation would be sensitive to changes in ribosome levels, we asked whether the increase in unbudded cells from Pwp2 depletion is a result of decreased Cln3 protein levels.

We disrupted the nonessential *CLN3* and asked if *cln3Δ* yeast also depleted of Pwp2 would accumulate unbudded cells. Pwp2-depleted yeast and the parent strain YPH499 in a *cln3Δ* or *CLN3* background were shifted into dextrose
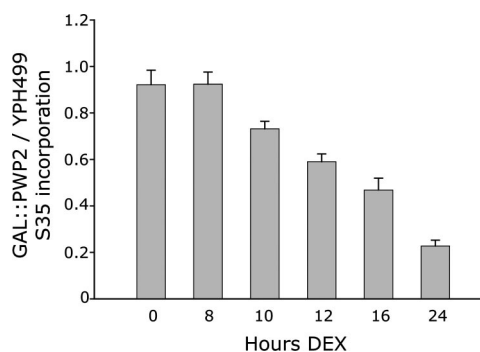


**Figure 3.** A decrease in new protein synthesis is not detectable until 10 h of Pwp2 depletion. *GAL::PWP2* and YPH499 were grown in medium containing galactose and raffinose as a carbon source and then shifted into medium containing glucose (DEX) for the indicated time periods. Cells were pulsed with Trans³⁵S-label, and TCA-precipitable protein was analyzed. ³⁵S-amino acid incorporation of *GAL::PWP2* cells was normalized for each experiment to the same time point in the control strain, YPH499. The ratios of three independent sets of experiments were averaged, and the SD was calculated.

media and monitored for growth. After 12 h of Pwp2 depletion, *cln3Δ* and YPH499 yeast exhibited comparably slowed growth based on OD600 (Figure 4A). Because Pwp2-depleted yeast accumulated G1 cells, we asked if *cln3Δ* Pwp2-depeleted yeast would behave similarly. The results showed that *cln3Δ* yeast accumulated unbudded cells with kinetics similar to that of *CLN3* yeast when Pwp2 was depleted, starting after ~8 h in dextrose (Figure 4A).

Because Pwp2 depletion leads to G1 delay and Cln3 is an important G1 regulator, we asked if reduced Cln3 protein levels accompany the accumulation of unbudded cells observed with Pwp2 depletion. To do this, *CLN3* was MYC tagged in a *GAL::3xHA-PWP2* strain using a tagging construct that has previously been used to visualize Cln3 by Western blot (Miller *et al.,* 2005). Correct tagging of Cln3 was verified by Western blotting with anti-Myc antibody. A single detectable Cln3 protein band ran at ~65 kDa, comigrating with a protein band in a previously characterized tagged Cln3 strain (Miller *et al.,* 2005). A band of that size was not detected in the untagged parent strain (YPH499; data not shown). Yeast depleted or not of Pwp2 were tested for Cln3, Pwp2, Mpp10, and Adh1 protein levels. As expected, Pwp2 protein levels were reduced after 4 h of depletion (Figure 4B). Cln3 protein levels, however, decreased only after 14 h of Pwp2 depletion (Figure 4B). Protein levels of Mpp10 (another known SSU processome component) and Adh1 (an unrelated abundant protein) did not change during this time course when Pwp2 was depleted (Figure 4B). Protein levels of the Cln3, Pwp2, Mpp10, and Adh1 proteins were unaffected when grown in YPG media (Figure 4B). Clearly, both the increase in unbudded cells and the slowing of growth precede the decrease in Cln3 protein levels. Therefore, consistent with our genetic results, a decrease in the levels of the Cln3 protein cannot be responsible for the G1 delay when Pwp2 is depleted.

### Deletion of whi5 Blunts the G1 Delay Observed in Pwp2 Depleted Yeast

One candidate for mediating the G1 delay in response to inhibition of ribosome biogenesis is the Whi5 protein, because it is a known negative regulator of Start (Jorgensen *et al.,* 2002; Costanzo *et al.,* 2004; de Bruin *et al.,* 2004). There-

A.



B.
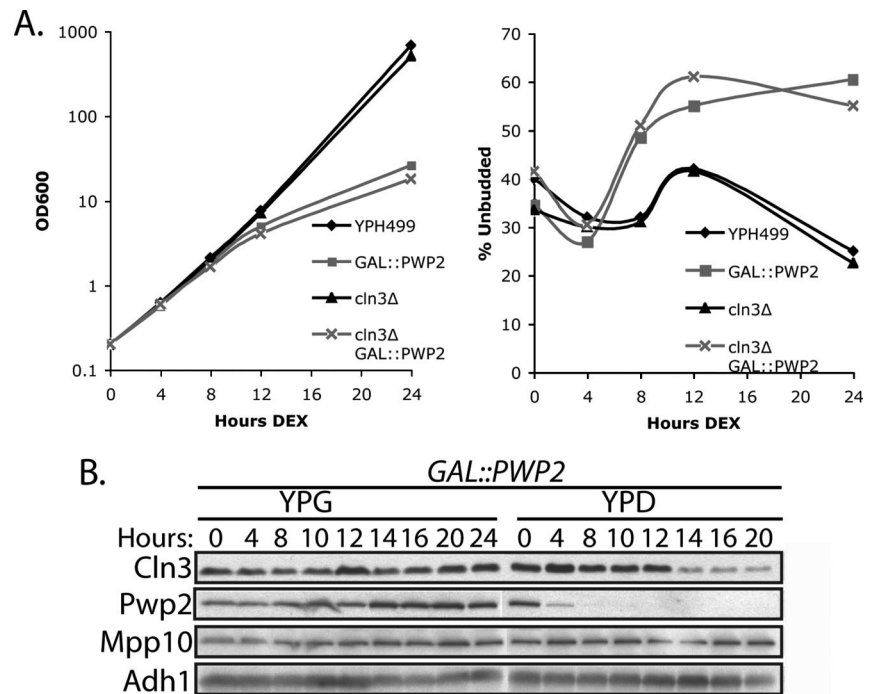


**Figure 4.** Accumulation of unbudded cells in Pwp2 depletion is Cln3 independent. (A) Cell growth and percentage of unbudded cells was monitored in *cln3Δ* Pwp2-depleted yeast. *GAL::PWP2 cln3Δ, cln3Δ, GAL::PWP2,* and the parent strain (YPH499) were grown in YPG media and then shifted into YPD. (B) Cln3 protein levels decrease after 14 h of Pwp2 depletion. Yeast with Cln3-HA-MYC tagged in a *GAL::3xHA-PWP2* strain was grown in YPG media and then maintained in early log phase in YPG or shifted into YPD media. Protein was extracted from an equal number of cells and analyzed by Western blot for Cln3 (anti-MYC antibodies), Pwp2 (anti-HA antibodies), Mpp10 (anti-Mpp10 antibodies), and Adh1 (anti-Adh1 antibodies) protein expression.

fore, we asked whether yeast with disrupted *WHI5* would accumulate unbudded cells when ribosome biogenesis is inhibited. Yeast with *GAL::PWP2 whi5Δ* or *whi5Δ* were shifted into dextrose media (Figure 5A). After 12 h in dextrose, yeast depleted of Pwp2 (*GAL::PWP2 whi5Δ*) slowed growth in comparison to *whi5Δ* (Figure 5A). Yeast were analyzed for changes in the cell cycle by 1) determining the percentage of unbudded cells and 2) analyzing cells by FACS. The results indicate that, in contrast to yeast where *WHI5* is intact, yeast depleted of Pwp2 when *WHI5* was disrupted did not accumulate unbudded or G1 cells with the same time course as yeast depleted of Pwp2 where *WHI5* was intact (Figure 5A). However, after extended Pwp2 depletion, *whi5Δ* yeast did accumulate unbudded cells, but to a limited extent (Figure 5A). Therefore, disrupting *WHI5* delays the G1 accumulation that is normally observed with Pwp2 depletion. Whi5 is thus likely involved in the initial cell cycle response, here examined at 8 h, to ribosome biogenesis defects. However, at later time points (24 h) when ribosome and protein levels are depleted and when protein synthesis is affected, a Whi5-independent mechanism likely ultimately causes G1 delay.

Because *GAL::PWP2* yeast when incubated in dextrose for 12 h were larger than the parent strain (YPH499), we asked whether *GAL::PWP2 whi5Δ* yeast were larger than *whi5Δ*. In contrast to Pwp2-depleted yeast, *whi5Δ* yeast did not significantly increase in cell size when Pwp2 was depleted for 24 h (Figure 5A). As expected from previously published results, *whi5Δ* yeast were smaller than the parent strain, YPH499 (Figure 5A and Supplementary Table 1; Jorgensen *et al.,* 2002; Costanzo *et al.,* 2004; de Bruin *et al.,* 2004).

Because yeast depleted of Pwp2 have less RNA per cell volume, we asked if *GAL::PWP2 whi5Δ* yeast would also have less RNA per cell volume when compared with *whi5Δ*. Cell elutriation was used to sort yeast by size depleted or not of Pwp2 for 12 h in a *whi5Δ* strain (Figure 5B). Yeast at the same budding index were compared for RNA or protein content per cell volume. The results indicate that *GAL::PWP2 whi5Δ* yeast incubated in dextrose were larger than *whi5Δ*

yeast at a budding index of 50% (Figure 5B). *GAL::PWP2 whi5Δ* yeast had a mode value volume of 42 fl, whereas *whi5Δ* cells had a mode value volume of 29 fl (Figure 5B; Supplementary Table 1). Therefore Pwp2-depleted cells were indeed larger than nondepleted cells when compared at the same budding index. These results suggest that although the accumulation of unbudded cells is delayed when *WHI5* is disrupted and Pwp2 depleted, *WHI5* disruption does not change the effects on cell size.

*GAL::PWP2 whi5Δ* yeast elutriated after incubation in dextrose for 12 h were analyzed for total RNA and protein content per cell volume as described previously for *GAL::PWP2* yeast. An elutriated fraction with 50% budded cells was used as a reference point. The results indicate that *GAL::PWP2 whi5Δ* yeast had a mode value of 367 RNA and 253 protein units, whereas *whi5Δ* cells had a mode value of 344 RNA and 258 protein units (Figure 5B). The results reveal that although *GAL::PWP2 whi5Δ* yeast are larger, they have roughly the same RNA and protein content when compared at the same budding index to *whi5Δ* yeast (Figure 5B; Supplementary Table 1).

### Whi5-GFP Increases Time Spent in the Nucleus in Pwp2-depleted Cells

Previously, it was determined that Whi5 can inhibit SBF/MBF while in the nucleus (Jorgensen *et al.,* 2002; Costanzo *et al.,* 2004; de Bruin *et al.,* 2004). To test whether deficiencies in ribosome biogenesis result in an increased interval of nuclear Whi5, expression of the Whi5-GFP protein was monitored in Pwp2-depleted (*GAL::PWP2*) and nondepleted (parent strain; W303) yeast by time-lapse microscopy (Bean *et al.,* 2006). By time-lapse microscopy of *WHI5-GFP* cells, growth of the mother cell (the cell before budding) and daughter cell (the bud on the mother cell) can be divided into three measurable intervals: 1) time from mother bud emergence to Whi5 nuclear entry (MBE-W5I), 2) time from Whi5 nuclear entry to Whi5 nuclear exit (W5I–W5O), and 3) time from Whi5 nuclear exit to bud emergence (W5O–BE; Figure 6A; Bean *et al.,* 2006). It is important to note that because we were unable to construct the
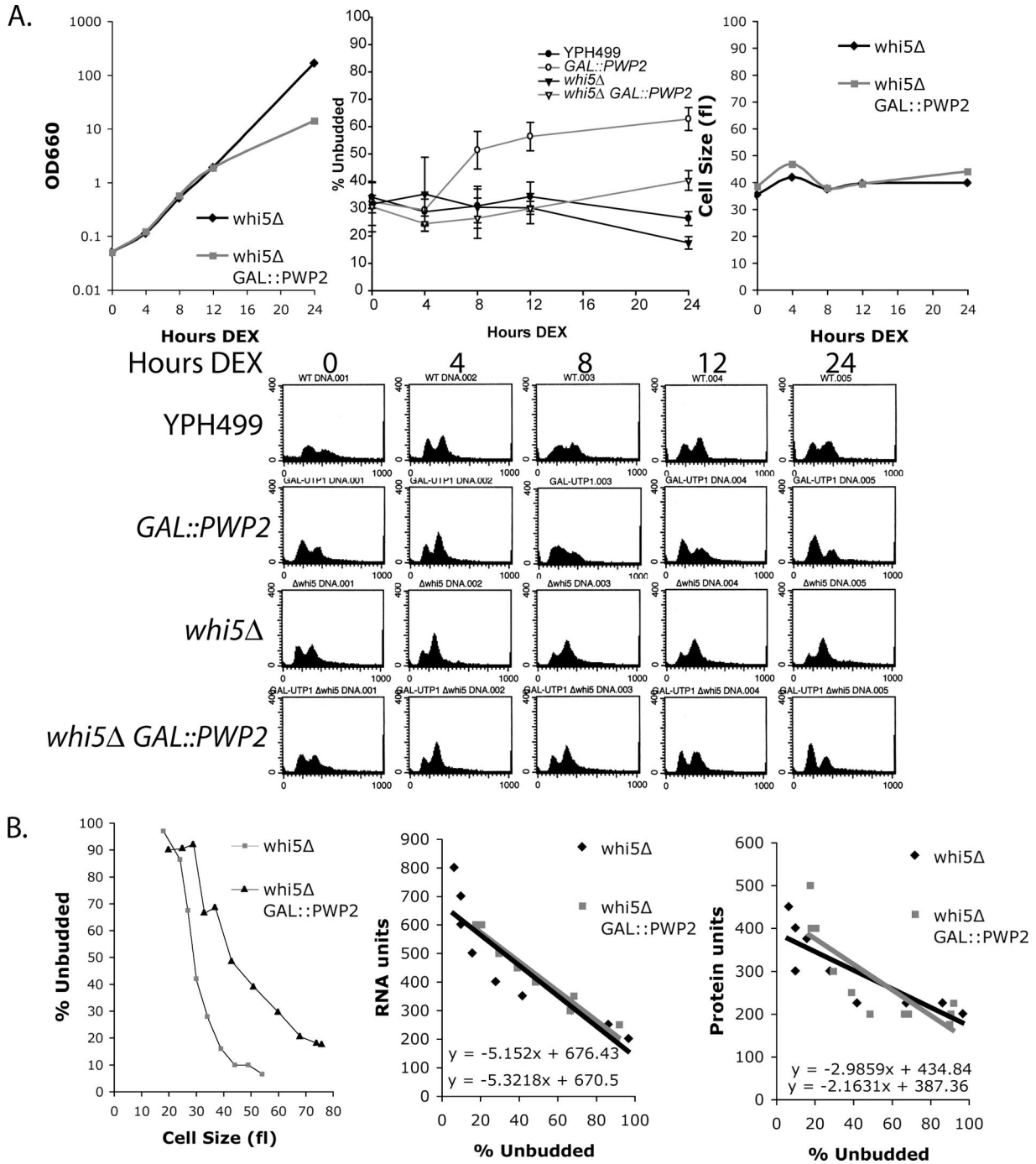
**Figure 5.** Cells with disrupted *WHI5* delay G1 arrest upon Pwp2 depletion. (A) Cell growth, percentage of unbudded cells, and cell size were monitored in *whi5*Δ Pwp2-depleted yeast. *GAL::PWP2 whi5*Δ and *whi5*Δ yeast were grown in YPG media and then shifted into YPD media. The same samples were also analyzed by FACS. The percentage of unbudded cells was averaged from three separate experiments, and the SD is indicated. The YPH499 and *GAL::PWP2* averages are superimposed from Figure 1B. Three of the four experiments were conducted simultaneously with the *whi5*Δ and *GAL::PWP2 whi5*Δ strains. (B) Elutriation of *whi5*Δ Pwp2-depleted yeast. *GAL::PWP2 whi5* or *whi5*Δ were grown in YPG and then shifted into YPD for 12 h. Cells were elutriated and analyzed for percentage of unbudded cells versus cell size, RNA units versus percentage of unbudded cells, or protein units versus percentage of unbudded cells.

Whi5-GFP strain in the YPH499 strain background, the time-lapse microscopy was conducted using the previously characterized Whi5-GFP strain in a W303 strain background (Bean *et al.*, 2006). W303 grows faster than the YPH499 strain background, thus altering the timing, but not the effects, of Pwp2 related cellular events (Supplementary Figure 1). The cell cycle

delay observed with Pwp2 depletion due to *whi5*Δ was also seen in W303, although the effect was less pronounced, perhaps because of the faster growth rate in W303 (data not shown).

To determine if Whi5 localization is altered upon inhibition of ribosome biogenesis, *GAL::PWP2* and *PWP2* (parent strain;
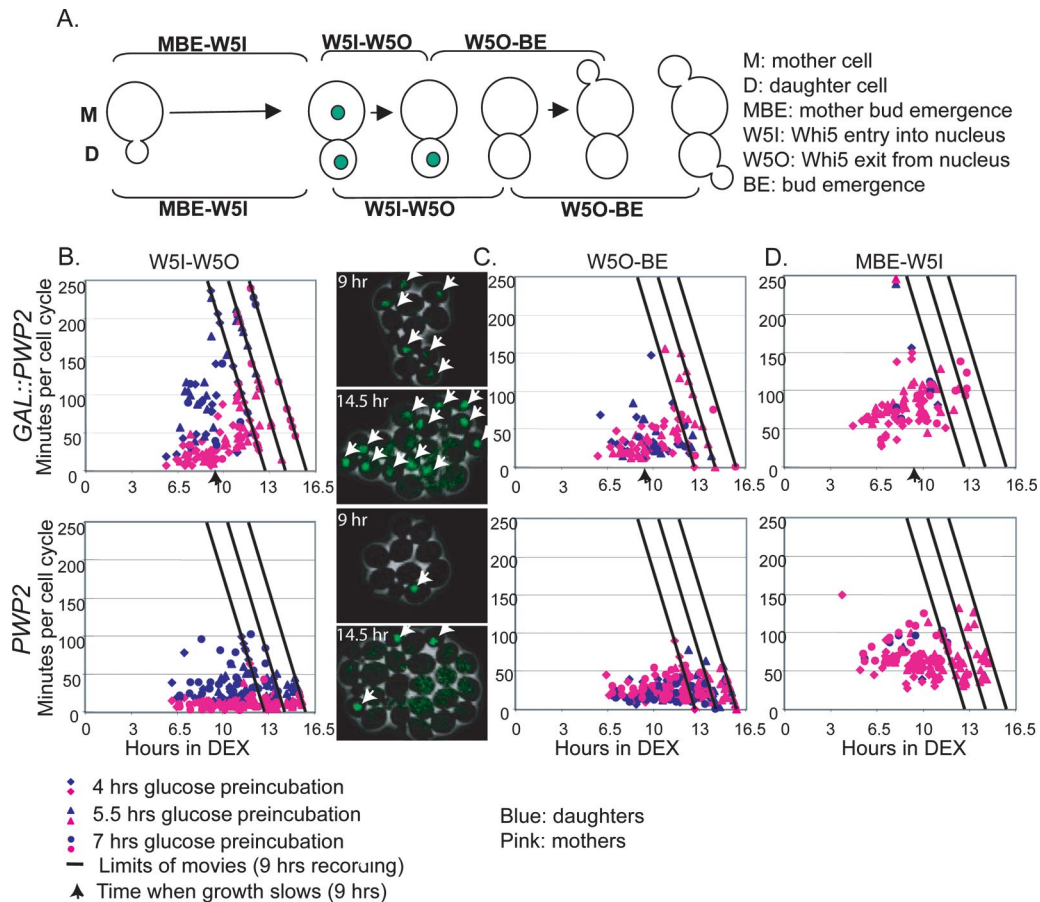
**Figure 6.** Increased nuclear residence time of Whi5 when ribosome biogenesis is disrupted. Using time-lapse microscopy, individual mother and daughter Whi5-GFP cells were analyzed in *GAL::PWP2* and *PWP2* yeast from a series of three movies representing different preincubation times in dextrose (either 4, 5.5, or 7 h). Data from all three movies were plotted on the same graph. The number of total hours in dextrose (Pwp2 depletion) is plotted on the *x*-axis and individual cell cycle interval is plotted on the *y*-axis in minutes. The time limit for each movie is shown with a diagonal line representing the maximum time for an event that could be observed. Uncompleted events, represented as symbols on the diagonal line, are assigned to the movie limit line. Individual mother cells are represented in pink, and daughter cells are blue. (A) Cell cycle analysis of individual Whi5-GFP yeast can be divided into three parts: 1) Mother bud emergence to Whi5 nuclear entry (MBE-W5I), 2) Whi5 nuclear entry to exit (W5I-W5O), and 3) Whi5 nuclear exit to bud emergence (W5O-BE). (B) Graph of time interval indicating Whi5 nuclear residence (W5I-W5O) in *GAL::PWP2* and *PWP2* yeast, as a function of time after transfer to dextrose that Whi5 nuclear entry occurred. Still frame examples of yeast depleted or not of Pwp2 (9 and 14.5 h dextrose) with nuclear Whi5-GFP foci marked with white arrows are from the 5.5 h dextrose preincubation movie. (C) Graph of time interval indicating Whi5 nuclear exit to bud emergence (W5O-BE) in *GAL::PWP2* and *PWP2* yeast, as a function of time after transfer to dextrose that Whi5 nuclear exit occurred. (D) Graph of the time interval indicating mother bud emergence to Whi5 nuclear entry (MBE-W5I) in *GAL::PWP2* and *PWP2*, as a function of time after transfer to dextrose that mother bud emergence occurred.

W303) yeast were preincubated in dextrose for varying intervals, plated on dextrose solid medium, and analyzed by time-lapse microscopy for Whi5-GFP nuclear entry/exit (Figure 6B). Three movies were analyzed, representing 4–16 h of growth in dextrose. Pwp2 depletion results in a steady increase in Whi5 nuclear residence time (W5I-W5O) in both the mother (pink) and daughter (blue) cells, with the increase beginning after ~6 h in dextrose (Figure 6B). In addition, by the completion of the movies, many cells still had nuclear Whi5 (indicated by points lying on the diagonal lines). Still images from the *GAL::PWP2* and *PWP2* movies (9 and 14.5 h dextrose) are shown with nuclear Whi5-GFP foci marked with white arrows as an example (Figure 6B). Whi5 nuclear entry-to-exit time was longer in wild-type daughter cells than in wild-type mother cells, as previously observed (Bean *et al.*, 2006). In Pwp2-depeleted yeast, consistent with our genetic results, increases in nuclear residence time of Whi5 occurs before the overt growth rate decreases (arrow in Figure 6B and Supplementary Figure 1).

Because Pwp2 depletion increases Whi5 nuclear retention time, we asked whether the time of bud emergence after Whi5 nuclear exit (W5O-BE) would also increase (Figure 6C). As previously observed (Figure 6C; Bean *et al.*, 2006), budding followed Whi5-GFP nuclear exit by ~25–30 min in *PWP2* yeast (Figure 6C). Pwp2-depleted yeast did not significantly change this interval when compared with *PWP2* yeast, at least until late in the depletion time course, significantly after clearly detectable increases in the Whi5 nuclear residence time (Figure 6C).

The range of time spent from mother bud emergence to Whi5 entry was similar for both *GAL::PWP2* and *PWP2* yeast, although some delay was detectable in the depleted cells late in the time course. Whi5 nuclear entry was simultaneous in both mother and daughter cells because of the sharing of common cytoplasm until mitotic exit (Figure 6D; Costanzo *et al.*, 2004; Bean *et al.*, 2006). In *GAL::PWP2* and *PWP2* cells, the interval between Whi5-GFP nuclear exit and
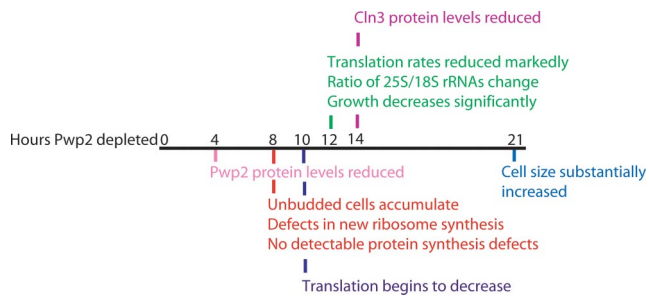
**Figure 7.** Timeline of cellular events that occur after Pwp2 depletion. 4 h, Pwp2 protein levels are reduced; 8 h, steady state pre-rRNAs accumulate, new ribosome synthesis is delayed, and unbudded cells accumulate; 10 h, new proteins synthesis begins to decrease; 12 h, ratio of 25S/18S increases, and translation and growth rates are significantly decreased; 14 h, Cln3 protein levels are reduced; and 21 h, cell size has substantially increased.

completion of mitosis, as indicated by Whi5-GFP nuclear reentry required ~40–120 min (Costanzo *et al.*, 2004; Bean *et al.*, 2006). These results indicate that upon inhibition of ribosome biogenesis, Whi5 nuclear residence time increases dramatically, before overt changes in cell growth rate, whereas other cell cycle intervals remain relatively unchanged until considerably later in the depletion time course.

## DISCUSSION

In the yeast *Saccharomyces cerevisiae*, cells must reach a critical size in order to progress through Start. How cells coordinate increases in cell size with cell cycle progression is not entirely known. Here we provide evidence that yeast can anticipate decreases in translation before they occur through regulation of Whi5, the yeast functional equivalent of the tumor suppressor Rb. Together, our results indicate that yeast sense whether ribosome biogenesis, and not the number of mature ribosomes, is adequate for cell cycle progression at the Start checkpoint.

To disrupt ribosome biogenesis we genetically depleted yeast of one protein that is required for SSU synthesis, Pwp2 (Dragon *et al.*, 2002; Dosil and Bustelo, 2004; Gallagher *et al.*, 2004), and monitored them for alterations (summarized in Figure 7). After 4 h, Pwp2 protein levels are visibly reduced (Figure 1A). After 8 h, defects in new ribosome synthesis (Figure 2, B–D), and an increase in unbudded cells (indicating G1 delay; Figure 1B) is observed. By 12 h of Pwp2 depletion, the growth rate has decreased (Figure 1B), translation rates are reduced (Figure 3), and the ratio of 25S/18S rRNAs is increased (indicating decreases in SSU; Figure 2C). By 14 h, Cln3 levels are decreased (Figure 4). By 21 h, cell size has substantially increased (Figure 1D). Whi5 retention in the nucleus accompanies increases in unbudded cells and pre-rRNA processing defects in the W303 strain (Figure 6B; Supplementary Figure 1). Because defects in cell cycle progression (Whi5 nuclear retention in W303 and increases in the percentage of unbudded cells) occur before a decrease in the number of functional ribosomes and translation, yeast may be sensing accumulation of 18S rRNA precursors or decreases in newly synthesized SSU subunits. Therefore, defects in ribosome biogenesis, and not decreases in the steady state number of functional ribosomal subunits, may be initially sensed at Start. Alternatively, yeast could be sensing a balance between new 60S and 40S subunit synthesis or decreases in new 40S subunit synthesis. In addition, we cannot exclude the possibility that yeast sense small

changes in translation that are undetectable with our assays because changes in translation can clearly influence Start (Unger and Hartwell, 1976; Moore, 1988).

A screen for nonessential genes whose disruption reduces cell size at budding yielded two transcription factors, Sfp1 and Sch9. These proteins activate expression of proteins involved in the RiBi and RP regulons (Jorgensen *et al.*, 2002, 2004a). Yeast sense nutrients and stress via the Ras/PKA and TOR signaling pathways which signal to Sfp1 and Sch9 to alter synthesis of RiBi and RP regulons (Jorgensen *et al.*, 2004a; Marion *et al.*, 2004). Jorgensen *et al.* hypothesized that adequate nutrients influence Start at the level of ribosome biogenesis rather than by alterations in the protein synthesis rate (Jorgensen and Tyers, 2004; Jorgensen *et al.*, 2004b). The mechanism of how Sfp1 and Sch9 couple ribosome biogenesis to Start through the SBF/MBF complexes is unknown, but it is thought that decreasing the rate of ribosome biogenesis lowers the critical size setpoint needed for budding. It has been hypothesized that these effects are independent of Cln3 and Whi5 because the cell size setpoint can be changed independently of *CLN3/WHI5* (Jorgensen *et al.*, 2004a).

Deficiencies in ribosome biogenesis in many eukaryotes have previously been shown to result in smaller cells (Shima *et al.*, 1998; Montagne *et al.*, 1999; Jorgensen *et al.*, 2002, 2004a; Oliver *et al.*, 2004; Ruvinsky *et al.*, 2005). These results suggest that limiting ribosome biogenesis causes cells to set the cell size setpoint at a smaller cell volume. Although Jorgensen *et al.* analyzed the effects of alterations in transcription factors that globally regulate many downstream targets, we examined this phenomenon by inhibiting ribosome biogenesis through genetic depletion of the SSU processome and therefore analyzed events that happen downstream of Sfp1 and Sch9. In contrast to Jorgensen *et al.* (2004a), we found that inhibiting ribosome biogenesis (by Pwp2 depletion) did not result in smaller cell volumes. Furthermore, yeast depleted of Utp10 (another SSU processome protein), Fap7 (a protein required for cytoplasmic 20S pre-rRNA processing), and Rpf1 (a protein required for LSU biogenesis) also resulted in larger cell volumes (data not shown). Our results suggest that the cell cycle defects that we observe after 12 h are not related to reduced growth in cell volume because the volume of our cells is larger and suggests that yeast may be sensing cell "size" through another parameter (or parameters) such as RNA content, protein content, cytoplasmic volume, or the ratio of cytoplasmic to nuclear volume. This is important as the mechanism by which yeast sense "size" for cell cycle progression has remained unclear (Jorgensen and Tyers, 2004).

One explanation for the differences between our results and those of Jorgensen *et al.* could be that we analyzed the effects of depleting essential proteins instead of disrupting nonessential genes (Shima *et al.*, 1998; Montagne *et al.*, 1999; Jorgensen *et al.*, 2002, 2004a; Oliver *et al.*, 2004; Ruvinsky *et al.*, 2005). Alternatively, we may have inhibited steps in ribosome biogenesis downstream of Sfp1 and Sch9, bypassing the mechanism that resets the cell size setpoint.

Although ribosome biogenesis may negatively regulate Start by increasing the cell size setpoint (Jorgensen *et al.*, 2002, 2004a), we found that ribosome biogenesis can also positively promote Start. Our results suggest that cells can independently sense alterations in rates of ribosome biogenesis at Start before overt decreases in ribosome number or protein synthesis. We found that adequate ribosome biogenesis is needed to promote Start and that this effect is mediated, at least in part, by Whi5. Thus ribosome biogenesis may positively regulate Start by somehow inhibiting Whi5.

Together these results suggest that ribosome biogenesis can have negative and positive regulatory roles on Start.

When we investigated why inhibition of ribosome biogenesis led to larger cells, we found that *GAL::PWP2* yeast had enlarged vacuoles. Vacuole enlargement can have a major impact on cell volume, and indeed, at least some of the increased cell size in *cln3* null cells (Cross, 1988; Nash *et al.,* 1988) is due to vacuolar enlargement (Han *et al.,* 2003, 2005). Vacuoles are analogous to mammalian lysosomes and function as a repository for metabolites and low-molecular-weight compounds. The enlarged vacuoles observed with Pwp2 depletion may be a result of cells undergoing autophagy or "self-eating" (Klionsky, 2005).

Because both Whi5 and Cln3 are important regulators of passage through Start (Jorgensen and Tyers, 2004; Jorgensen *et al.,* 2004b), we hypothesized that these proteins might be mediating the cell cycle effects observed upon inhibition of ribosome biogenesis. Our results indicate that when ribosome biogenesis is inhibited by Pwp2 depletion, the Whi5 protein becomes retained in the nucleus, where it might contribute to delay of Start. Consistently, the G1 delay observed with Pwp2 depletion is delayed by *whi5* deletion. Therefore, the initial response to ribosome biogenesis defects may occur through a Whi5-dependent mechanism. Alternatively, increased nuclear Whi5 could be a result, and not the cause, of the cell cycle defects observed. In any case, the genetic results that Whi5 is required for the cell cycle response (Figure 5) indicated that Whi5 is involved at some level. Although one role of Cln3 is to phosphorylate Whi5 to regulate its subcellular localization, our results suggest that defects in ribosome biogenesis leading to G1 delay occur independently of Cln3 protein levels. However, we cannot rule out the possibility that undetectably small changes in Cln3 protein levels or its modifications can result from Pwp2 depletion at earlier time points. Collectively, our genetic results suggest that the cell cycle defects observed with Pwp2 depletion were independent of Cln3 levels and dependent on Whi5. The genetic data were further supported by the observation that decreases in Cln3 protein levels occur both after the cell cycle defects and alterations in the cellular localization of Whi5 were observed. Therefore, there may be another labile cell cycle regulator that negatively regulates Whi5 in response to defects in ribosome biogenesis.

Our findings suggest that Whi5 is involved in coordinating adequate ribosome synthesis to G1 cell cycle progression. Whi5 is the yeast functional equivalent to the tumor suppressor Rb. This family of tumor suppressor genes is mutated in many types of cancers and is important in regulation of rRNA synthesis (Ruggero and Pandolfi, 2003). Several studies show a close relationship between Rb and transcription of the rDNA by RNA polymerase I (Cavanaugh *et al.,* 1995; Hannan *et al.,* 2000; Ciarmatori *et al.,* 2001), and deleting Rb leads to increases in rRNA synthesis (Ciarmatori *et al.,* 2001). Thus Whi5 and Rb have roles in both ribosome biogenesis and Start, although the regulatory connections may differ. In the future, it will be interesting to know if the analogy between Whi5 and Rb can be extended to the response to (and perhaps even regulation of) ribosome biogenesis.

## ACKNOWLEDGMENTS

## REFERENCES

Bean, J. M., Siggia, E. D., and Cross, F. R. (2006). Coherence and timing of cell cycle start examined at single-cell resolution. Mol. Cell *21*, 3–14.

Bernstein, K. A., and Baserga, S. J. (2004). The small subunit processome is required for cell cycle progression at G1. Mol. Biol. Cell *15*, 5038–5046.

Bernstein, K. A., Gallagher, J. E., Mitchell, B. M., Granneman, S., and Baserga, S. J. (2004). The small-subunit processome is a ribosome assembly intermediate. Eukaryot. Cell *3*, 1619–1626.

Burton, J. L., and Solomon, M. J. (2000). Hsl1p, a Swe1p inhibitor, is degraded via the anaphase-promoting complex. Mol. Biol. Cell *20*, 4614–4625.

Cavanaugh, A. H., Hempel, W. M., Taylor, L. J., Rogalsky, V., Todorov, G., and Rothblum, L. I. (1995). Activity of RNA polymerase I transcription factor UBF blocked by Rb gene product. Nature *374*, 177–180.

Ciarmatori, S., Scott, P. H., Sutcliffe, J. E., McLees, A., Alzuherri, H. M., Dannenberg, J. H., te Riele, H., Grummt, I., Voit, R., and White, R. J. (2001). Overlapping functions of the pRb family in the regulation of rRNA synthesis. Mol. Cell. Biol. *21*, 5806–5814.

Costanzo, M., Nishikawa, J. L., Tang, X., Millman, J. S., Schub, O., Breitkreuz, K., Dewar, D., Rupes, I., Andrews, B., and Tyers, M. (2004). CDK activity antagonizes Whi5, an inhibitor of G1/S transcription in yeast. Cell *117*, 899–913.

Cross, F. R. (1988). DAF1, a mutant gene affecting size control, pheromone arrest, and cell cycle kinetics of *Saccharomyces cerevisiae.* Mol. Cell. Biol. *8*, 4675–4684.

Cross, F. R., and Blake, C. M. (1993). The yeast Cln3 protein is an unstable activator of Cdc28. Mol. Cell. Biol. *13*, 3266–3271.

de Bruin, R. A., McDonald, W. H., Kalashnikova, T. I., Yates, J., 3rd, and Wittenberg, C. (2004). Cln3 activates G1-specific transcription via phosphorylation of the SBF bound repressor Whi5. Cell *117*, 887–898.

Dolznig, H., Grebien, F., Sauer, T., Beug, H., and Mullner, E. W. (2004). Evidence for a size-sensing mechanism in animal cells. Nat. Cell Biol. *6*, 899–905.

Donachie, W. D. (1968). Relationship between cell size and time of initiation of DNA replication. Nature *219*, 1077–1079.

Dosil, M., and Bustelo, X. R. (2004). Functional characterization of Pwp2, a WD family protein essential for the assembly of the 90 S pre-ribosomal particle. J. Biol. Chem. *279*, 37385–37397.

Dragon, F. *et al.* (2002). A large nucleolar U3 ribonucleoprotein required for 18S ribosomal RNA biogenesis. Nature *417*, 967–970.

Du, Y. C., and Stillman, B. (2002). Yph1p, an ORC-interacting protein: potential links between cell proliferation control, DNA replication, and ribosome biogenesis. Cell *109*, 835–848.

Dunbar, D. A., Wormsley, S., Agentis, T. M., and Baserga, S. J. (1997). Mpp10p, a U3 small nucleolar ribonucleoprotein component required for pre-18S rRNA processing in yeast. Mol. Cell. Biol. *17*, 5803–5812.

Fingerman, I., Nagaraj, V., Norris, D., and Vershon, A. K. (2003). Sfp1 plays a key role in yeast ribosome biogenesis. Eukaryotic Cell *2*, 1061–1068.

Gallagher, J. E., Dunbar, D. A., Granneman, S., Mitchell, B. M., Osheim, Y., Beyer, A. L., and Baserga, S. J. (2004). RNA polymerase I transcription and pre-rRNA processing are linked by specific SSU processome components. Genes Dev. *18*, 2506–2517.

Goldstein, A. L., and McCusker, J. H. (1999). Three new dominant drug resistance cassettes for gene disruption in *Saccharomyces cerevisi*ae. Yeast *15*, 1541–1553.

Grandi, P. *et al.* (2002). 90S pre-ribosome include the 35S pre-rRNA, the U3 snoRNP, and 40S subunit processing factors but predominantly lack 60S synthesis factors. Mol. Cell *10*, 105–115.

Han, B. K., Aramayo, R., and Polymenis, M. (2003). The G1 cyclin Cln3p controls vacuolar biogenesis in *Saccharomyces cerevisiae.* Genetics *165*, 467–476.

Han, B. K., Bogomolnaya, L. M., Totten, J. M., Blank, H. M., Dangott, L. J., and Polymenis, M. (2005). Bem1p, a scaffold signaling protein, mediates cyclin-dependent control of vacuolar homeostasis in *Saccharomyces cerevisiae.* Genes Dev. *19*, 2606–2618.

Hannan, K. M., Kennedy, B. K., Cavanaugh, A. H., Hannan, R. D., Hirschler-Laszkiewicz, I., Jefferson, L. S., and Rothblum, L. I. (2000). RNA polymerase

I transcription in confluent cells: Rb downregulates rDNA transcription during confluence-induced cell cycle arrest. Oncogene *19*, 3487–3497.

Hartwell, L. H., Culotti, J., Pringle, J. R., and Reid, B. J. (1974). Genetic control of the cell division cycle in yeast. Science *183*, 46–51.

Hartwell, L. H., and Unger, M. W. (1977). Unequal division in *Saccharomyces cerevisiae* and its implications for the control of cell division. J. Cell Biol. *75*, 422–435.

Johnston, G. C., Pringle, J. R., and Hartwell, L. H. (1977). Coordination of growth with cell division in the yeast *Saccharomyces cerevisiae*. Exp. Cell Res. *105*, 79–98.

Jorgensen, P., Nishikawa, J. L., Breitkreutz, B. J., and Tyers, M. (2002). Systematic identification of pathways that couple cell growth and division in yeast. Science *297*, 395–400.

Jorgensen, P., Rupes, I., Sharom, J. R., Schneper, L., Broach, J. R., and Tyers, M. (2004a). A dynamic transcriptional network communicates growth potential to ribosome synthesis and critical cell size. Genes Dev. *18*, 2491–2505.

Jorgensen, P., and Tyers, M. (2004). How cells coordinate growth and division. Curr. Biol. *14*, R1014–1027.

Jorgensen, P., Tyers, M., and Warner, J. R. (2004b). Forging the factory: ribosome synthesis and growth control in budding yeast. In: Cell Growth, ed., M. N. Hall, M. Raff, G. Thomas, New York: Cold Spring Harbor Laboratory Press, 329–370.

Klionsky, D. J. (2005). Autophagy. Curr. Biol. *15*, R282–R283.

Kushnirov, V. V. (2000). Rapid and reliable protein extraction from yeast. Yeast *16*, 857–860.

Lee, S. J., and Baserga, S. J. (1997). Functional separation of pre-rRNA processing steps revealed by truncation of the U3 small nucleolar ribonucleoprotein component, Mpp10. Proc. Natl. Acad. Sci. USA *94*, 13536–13541.

Lee, S. J., and Baserga, S. J. (1999). Imp3p and Imp4p: two specific components of the U3 small nucleolar ribonucleoprotein that are essential for pre-18S rRNA processing. Mol. Cell. Biol. *19*, 5441–5452.

Longtine, M. S., McKenzie, A. R., Demarini, D. J., Shah, N. G., Wach, A., Brachat, A., Philippsen, P., and Pringle, J. R. (1998). Additional modules for versatile and economical PCR-based gene deletion and modification in *Saccharomyces cerevisiae*. Yeast *14*, 953–961.

Marion, R. M., Regev, A., Segal, E., Barash, Y., Koller, D., Friedman, N., and O'Shea, E. K. (2004). Sfp1 is a stress- and nutrient-sensitive regulator of ribosomal protein gene expression. Proc. Natl. Acad. Sci. USA *101*, 14315–14322.

Miller, M. E., Cross, F. R., Groeger, A. L., and Jameson, K. L. (2005). Identification of novel and conserved functional and structural elements of the G1 cyclin Cln3 important for interactions with the CDK Cdc28 in *Saccharomyces cerevisiae*. Yeast *22*, 1021–1036.

Montagne, J., Stewart, M. J., Stocker, H., Hafen, E., Kozma, S. C., and Thomas, G. (1999). *Drosophila* S6 kinase: a regulator of cell size. Science *285*, 2126–2129.

Moore, S. A. (1988). Kinetic evidence for a critical rate of protein synthesis in the *Saccharomyces cerevisiae* yeast cell cycle. J. Biol. Chem. *263*, 9674–9681.

Nash, R., Tokiwa, G., Anand, S., Erickson, K., and Futcher, A. B. (1988). The WHI1+ gene of *Saccharomyces cerevisiae* tethers cell division to cell size and is a cyclin homolog. EMBO J. *7*, 4335–4346.

Nurse, P., and Thuriaux, P. (1977). Controls over the timing of DNA replication during the cell cycle of fission yeast. Exp. Cell Res. *107*, 365–375.

Oeffinger, M., and Tollervey, D. (2003). Yeast Nop15p is an RNA-binding protein required for pre-rRNA processing and cytokinesis. EMBO J. *22*, 6573–6583.

Oliver, E. R., Saunders, T. L., Tarle, S. A., and Glaser, T. (2004). Ribosomal protein L24 defect in belly spot and tail (Bst), a mouse Minute. Development *131*, 3907–3920.

Pestov, D. G., Stockelman, M. G., Strezoska, Z., and Lau, L. F. (2001a). ERB1, the yeast homolog of mammalian Bop1, is an essential gene required for maturation of the 25S and 5.8S ribosomal RNAs. Nucleic Acids Res. *29*, 3621–3630.

Pestov, D. G., Strezoska, Z., and Lau, L. F. (2001b). Evidence of p53-dependent cross-talk between ribosome biogenesis and the cell cycle: effects of nucleolar protein Bop1 on G(1)/S transition. Mol. Cell. Biol. *21*, 4246–4255.

Polymenis, M., and Schmidt, E. V. (1997). Coupling of cell division to cell growth by translational control of the G1 cyclin CLN3 in yeast. Genes Dev. *11*, 2522–2531.

Popolo, L., Vanoni, M., and Alberghina, L. (1982). Control of the yeast cell cycle by protein synthesis. Exp. Cell Res. *142*, 69–78.

Ruggero, D., and Pandolfi, P. P. (2003). Does the ribosome translate cancer? Nat. Rev. Cancer *3*, 179–192.

Ruvinsky, I., Sharon, N., Lerer, T., Cohen, H., Stolovich-Rain, M., Nir, T., Dor, Y., Zisman, P., and Meyuhas, O. (2005). Ribosomal protein S6 phosphorylation is a determinant of cell size and glucose homeostasis. Genes Dev. *19*, 2199–2211.

Saracino, F., Bassler, J., Muzzini, D., Hurt, E., and Carbone, M.L.A. (2004). The yeast kinase Swe1 is required for proper entry into cell cycle after arrest due to ribosome biogenesis and protein synthesis defects. Cell Cycle *3*, 648–654.

Schäfer, T., Straub, D., Petfalski, E., Tollervey, D., and Hurt, E. (2003). The path from nucleolar 90S to cytoplasmic 40S pre-ribosomes. EMBO J. *22*, 1370–1380.

Shima, H., Pende, M., Chen, Y., Fumagalli, S., Thomas, G., and Kozma, S. C. (1998). Disruption of the p70(s6k)/p85(s6k) gene reveals a small mouse phenotype and a new functional S6 kinase. EMBO J. *17*, 6649–6659.

Strezoska, Z., Pestov, D. G., and Lau, L. F. (2002). Functional inactivation of the mouse nucleolar protein Bop1 inhibits multiple steps in pre-rRNA processing and blocks cell cycle progression. J. Biol. Chem. *277*, 29617–29625.

Tyers, M., Tokiwa, G., and Futcher, B. (1993). Comparison of the *Saccharomyces cerevisiae* G1 cyclins: Cln3 may be an upstream activator of Cln1, Cln2 and other cyclins. EMBO J *12*, 1955–1968.

Tyers, M., Tokiwa, G., Nash, R., and Futcher, B. (1992). The Cln3-Cdc28 kinase complex of *S. cerevisiae* is regulated by proteolysis and phosphorylation. EMBO J. *11*, 1773–1784.

Unger, M. W., and Hartwell, L. H. (1976). Control of cell division in *Saccharomyces cerevisiae* by methionyl-tRNA. Proc. Natl. Acad. Sci. USA *73*, 1664–1668.

Wijnen, H., and Futcher, B. (1999). Genetic analysis of the shared role of CLN3 and BCK2 at the G(1)-S transition in *Saccharomyces cerevisiae*. Genetics *153*, 1131–1143.